The Proton/Amino Acid Cotransporter PAT2 Is Expressed in Neurons with a Different Subcellular Localization than Its Paralog PAT1*

Received for publication, May 28, 2003, and in revised form, September 24, 2003 Published, JBC Papers in Press, November 3, 2003, DOI 10.1074/jbc.M305556200

Isabel Rubio-Aliaga‡\$¶, Michael Boll‡¶, Daniela M. Vogt Weisenhorn∥, Martin Foltz‡, Gabor Kottra‡, and Hannelore Daniel‡**

From the ‡Molecular Nutrition Unit, Technical University of Munich, Hochfeldweg 2, D-85350 Freising-Weihenstephan, Germany and the ||National Research Center, Institute of Developmental Genetics, Ingostädter Landstrasse 1, D-85764 Neuherberg, Germany

The new member of the mammalian amino acid/auxin permease family, PAT2, has been cloned recently and represents an electrogenic proton/amino acid symporter. PAT2 and its paralog, PAT1/LYAAT-1, are transporters for small amino acids such as glycine, alanine, and proline. Our immunodetection studies revealed that the PAT2 protein is expressed in spinal cord and brain. It is found in neuronal cell bodies in the anterior horn in spinal cord and in brain stem, cerebellum, hippocampus, hypothalamus, rhinencephalon, cerebral cortex, and olfactory bulb in the brain. PAT2 is expressed in neurons positive for the N-methyl-D-aspartate subtype glutamate receptor subunit NR1. PAT2 is not found in lysosomes, unlike its paralog PAT1, but is present in the endoplasmic reticulum and recycling endosomes in neurons. PAT2 has a high external proton affinity causing half-maximal transport activation already at a pH of 8.3, suggesting that its activity is most likely not altered by physiological pH changes. Transport of amino acids by PAT2 activity is dependent on membrane potential and can occur bidirectionally; membrane depolarization causes net glycine outward currents. Our data suggest that PAT2 contributes to neuronal transport and sequestration of amino acids such as glycine, alanine, and/or proline, whereby the transport direction is dependent on the sum of the driving forces such as substrate concentration, pH gradient, and membrane potential.

The amino acid/auxin permease (AAAP)¹ family is one of the largest families of amino acid transporters identified so far, with members found in virtually all eukaryotic organisms (1–3). Hitherto, three different subfamilies of the AAAP transporters have been identified in mammals as represented by the

following: (a) the vesicular GABA transporter (VGAT) (4, 5); (b) the system A/N subfamily (6-10); and (c) the recently described proton/amino acid transporter (PAT) subfamily (11, 12). Although there is no pronounced sequence similarity among the AAAP transporters, they all recognize certain amino acids or closely related compounds and are highly sensitive to alterations in intracellular or extracellular proton concentrations.

The first mammalian AAAP transporter identified was the vesicular GABA transporter VGAT, also designated the vesicular inhibitory amino acid transporter (VIAAT). VGAT mediates the transport of the two inhibitory neurotransmitters, GABA and glycine, and appears to be expressed solely in the brain. As a neurotransmitter/proton antiporter (4, 5), it plays a crucial role in glycinergic and GABAergic transmission by accumulation of glycine and GABA in secretory vesicles in presynaptic nerve terminals.

The second subfamily comprises three different types of system A transporters (SAT1–3/ATA1–3) and two types of system N transporters (SN1 and SN2) (6–10, 13). Both classes play important roles in the homeostasis of various neutral amino acids in different tissues. Particularly in the brain system, A and N transporters possess a central role in the glutamate-glutamine cycle between astrocytes and neurons involved in recycling glutamate for its role in neurotransmission (14). Both systems are Na⁺-dependent co-transporters but differ with respect to the role of protons in the transport process. System N mediates H⁺ efflux during Na⁺-dependent amino acid influx (9), whereas system A members do not translocate protons, although their activity is markedly affected by the extracellular proton concentration (15).

The third mammalian AAAP subfamily is represented by the PAT1 to PAT4 proteins that were cloned recently (3, 11, 12). PAT3 and PAT4 are orphan transporters, whereas PAT1 (also designated as LYAAT1) and PAT2 are characterized as electrogenic amino acid/proton co-transporters with a high selectivity for amino acids with apolar and small side chains (3, 16). PAT1 was shown to transport glycine, L-alanine, and L-proline as well as GABA and D-serine (11, 12, 17–19). It is present in almost all tissues analyzed and shows high expression levels in brain, small intestine, kidney, and colon. In brain, PAT1 is mainly found in lysosomes in neurons, where it is involved in proton-driven export of amino acids from lysosomal protein breakdown (11). To some extent, PAT1 is also found in the plasma membrane (19).

Here we report that, like the other mammalian members of the AAAP family, PAT2 is well expressed in the central nervous system and is found predominantly in recycling endosomes and in the endoplasmic reticulum in neurons. Furthermore, we

 $^{^{\}ast}$ This research was supported by Deutsche Forschungsgemeinschaft (FSG) Grant BO 1857/1 (to M. B.). The costs of publication of this article were defrayed in part by the payment of page charges. This article must therefore be hereby marked "advertisement" in accordance with 18 U.S.C. Section 1734 solely to indicate this fact.

[§] Present address: Division of Hematology, Children's Hospital, Harvard Medical School, 300 Longwood Ave., Boston, MA 02115.

[¶] These authors contributed equally to this work.

^{**} To whom correspondence should be addressed. Tel.: 49-8161-713400; Fax: 49-8161-713999; E-mail: daniel@wzw.tum.de.

¹ The abbreviations used are: AAAP, amino acid/auxin permease; PAT, proton/amino acid transporter; LYAAT, lysosomal amino acid transporter; GABA, y-aminobutyric acid; VGAT, vesicular GABA transporter; RT, reverse transcription; GAPDH, glyceraldehyde-3-phosphate dehydrogenase; TBS, Tris-buffered saline; TEVC, two-electrode voltage clamp; GLYT, glycine transporter; NMDA, N-methyl-p-aspartate; NR, NMDA receptor; GAD65/67, glutamate decarboxylase 65/67.

demonstrate that transport activity of PAT2 is dependent on external pH and membrane potential and that the protein has the ability to transport in the reverse mode.

EXPERIMENTAL PROCEDURES

RNA Isolation and RT-PCR—Total RNA from different mouse brain regions (olfactory bulb, cortex, thalamus, cerebellum, and brain stem) and spinal cord was isolated with RNAwiz (Ambion), following the supplier's protocol. 5 μg of total RNA were reverse transcribed by using oligo(dT) as primer and the Retroscript kit (Ambion). 2 μl of each RT reaction were subjected to PCR reactions with the following primer pairs: 1) PAT2-F1 (5'-ATG TCT GTG ACC AAG AGT GCC-3') and PAT2-B546 (5'-GCA GCT GAT GGT TGT GCT GTT-3'); and 2) GAPDH-F (5'-GAC CAC AGT CCA TGA CAT CAC T-3') and GAPDH-B (5'-TCC ACC ACC CTG TTG CTG TAG-3'). PCR conditions were 94 °C for 1 min and 30 \times (94 °C for 30 s, 58 °C for 30 s, and 72 °C for 45 s).

Anti-PAT2 Antibody Production and Western Blot—A polyclonal antibody raised against the peptide CLDLIKSGNSPAL (amino acid residues 457–469 of the mouse PAT2 protein, GenBank™ accession number AAM80481) with the N-terminal cysteine coupled to keyhole limpet hemocyanin was produced in rabbit (Davids Biotechnologie). The antibody was affinity-purified on the peptide linked to Affi-Gel.

For Western blot analysis, 50 μg of crude protein prepared from mouse brain was separated by 10% SDS-PAGE followed by transfer onto a polyvinylidene difluoride membrane by using a semi-dry blotter (Bio-Rad). After blocking, the blot was immunostained with the anti-PAT2 antibody diluted 1:500 or the pre-absorbed antibody with the corresponding antigenic peptide. After washing with TBS, the blots were incubated with a horseradish peroxidase-conjugated anti-rabbit IgG antibody (1:1000; Dianova) and detected by 3-amino-9-ethyl-carbazole staining.

Heterologous Expression of PAT2 in Xenopus laevis Oocytes—Oocytes were handled as described previously (12), and either 25 nl (25 ng) of the mouse PAT2-cRNA or 25 nl of water (control) were injected into individual cells. Transport studies were performed 3 days after injection, as described previously (12). The two-electrode voltage clamp (TEVC) experiments were performed as reported (20). Briefly, steady state current-voltage (I-V) relationships were measured in incubation buffer (100 mm choline chloride or sodium chloride, 2 mm KCl, 1 mm MgCl₂, 1 mm CaCl₂, and 10 mm Tris at pH 7.5–9) in the absence or presence of glycine. Oocytes were clamped at -60 mV, and I-V relations were measured using short (100 ms) pulses separated by 200-ms pauses in the potential range of -160 to 80 mV. All values are expressed as mean \pm S.E.

Giant patch clamp experiments were performed as described previously (20) with patch pipettes filled with 10 mm NaCl, 80 mm sodium isethionate, 1 mm MgSO $_4$, 1 mm Ca(NO $_3$) $_2$, and 10 mm HEPES (pH 7.5) and an incubation buffer comprised of 100 mm potassium aspartate, 20 mm KCl, 4 mm MgCl $_2$, 2 mm EGTA, and 10 mm HEPES (pH 7.5) containing nothing or 20 mm glycine on the patch cytosolic surface. During perfusion, the membrane potential was clamped to -30 mV, and I-V relations in the potential range of -80 to 60 mV were measured in the same way as described for TEVC. For immunolocalization in occytes, cells injected with the PAT2-cRNA were initially checked for expression of the transporter by measuring positive inward currents induced by 20 mm glycine using the TEVC method. Oocytes were then fixed in 4% paraformaldehyde for 15 min at room temperature and processed for embedment in paraffin wax. Deparaffinized sections (10 μ m) were used for immunofluorescence analysis.

Immunodetection Studies-Immunohistochemistry and immunofluorescence detection of PAT2 were performed on deparaffinized brain or spinal cord sections from adult mouse transcardially perfused for 15 min with 4% paraformaldehyde in buffer 1 (100 mm sucrose, 100 mm NaCl, and 10 mm HEPES, pH 7.4) and washed for 5 min with buffer 1. Tissues were processed for embedding in paraffin wax. Antigen retrieval was carried out by incubating the slices in citrate buffer (pH 6) in a microwave oven. For immunohistochemistry, 5-µm sections were blocked for 20 min with 3% goat serum in TBS and incubated overnight with the affinity-purified anti-PAT2 antibody diluted 1:100. On the following day, sections were rinsed with TBS and incubated for 30 min with biotinylated goat anti-rabbit immunoglobulins (1:800; Dako), rinsed with TBS, and incubated for 30 min with peroxidase-conjugated streptavidin (1:300; Dako). After washing with TBS, the sections were stained for 5-10 min with DAB peroxidase substrate (Sigma). Control incubations in parallel sections were carried out by pre-absorption of the primary antibody with the corresponding antigenic peptide. For immunofluorescence analysis, 10-µm sections were blocked for 20 min

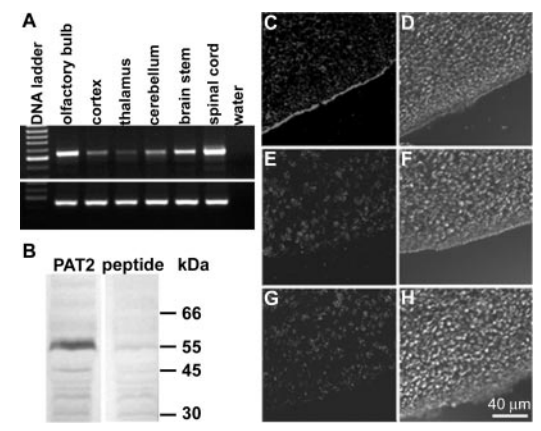


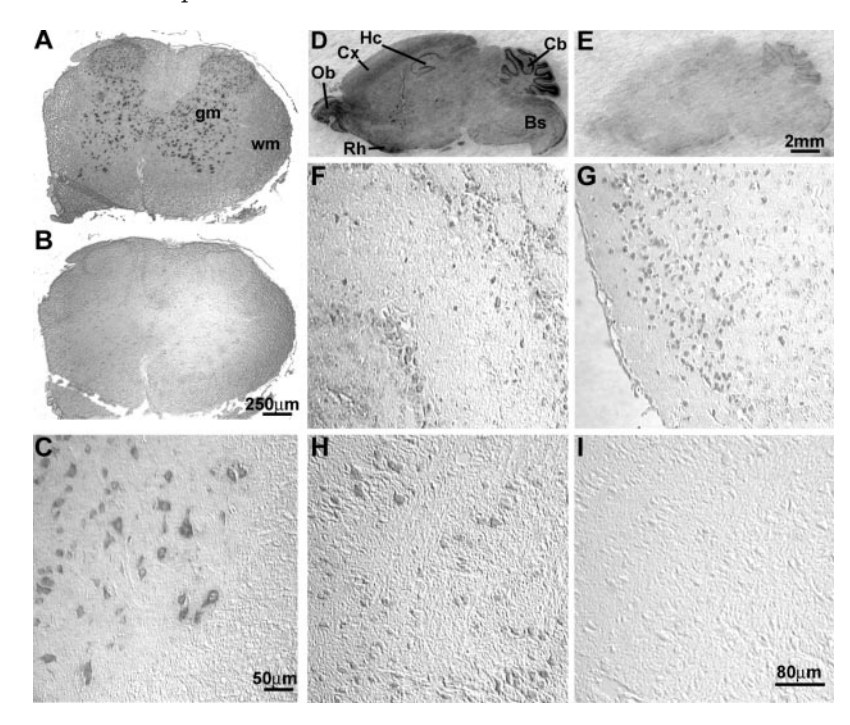
Fig. 1. Detection of PAT2 mRNA and protein in mouse brain and determination of anti-PAT2 antibody specificity. A, the RT-PCR analysis was performed with 5 μ g of total RNA extracted from the different brain regions indicated and water as a negative control. In the PCR reaction, PAT2-cDNA-specific primers were used to detect mRNA (top). The expected size of the product was 546 bp. As a control for RNA integrity, the GAPDH PCR product was amplified (bottom; expected size, 453 bp). B, the Western blot analysis was performed with a crude protein preparation isolated from murine brain and incubated with an anti-PAT2 antibody (left) or the antibody pre-absorbed with the antigenic peptide (right). C-H, for determination of anti-PAT2 antibody specificity, immunofluorescence studies were performed with 10-µm slices of X. laevis oocytes injected with PAT2-cRNA (C) or X. laevis oocytes injected with water (E) and incubated with the anti-PAT2 antibody. An additional control was performed by incubating 10-µm slices of X. laevis oocytes injected with PAT2-cRNA with the pre-absorbed anti-PAT2 antibody (E). D, F, and H are phase-contrast micrographs of C, E, and G, respectively. Scale bar in H applies to C–H.

with 3% goat serum and incubated overnight with the affinity-purified anti-PAT2 antibody diluted 1:100 or the affinity-purified anti-LYAAT-1 (1:500; kindly provided by B. Giros, INSERM U513, Créteil, France). Colocalization analysis was performed with 10-µm sections incubated overnight with the affinity-purified anti-PAT2 antibody diluted 1:100 and mouse anti-BiP/GRP78, mouse anti-GM130, mouse anti-Rab4, mouse anti-EEA1 (all diluted 1:50; BD Transduction Laboratories), goat anti-NR1, goat anti-gephyrin, goat anti-GAD65/67 (all diluted 1:25; Santa Cruz Biotechnology), or goat anti-GLYT2 (1:250; Chemicon). Slices were rinsed with TBS and incubated for 30 min with the following: (a) Cy3-conjugated donkey anti-rabbit IgG (1:800; Dianova) and Alexa Fluor 633 goat anti-mouse IgG (1:1000; Molecular Probes); or (b) Cy5-conjugated donkey anti-rabbit IgG (1:500; Dianova) and Alexa Fluor 488-conjugated donkey anti-goat IgG (1:500; Molecular Probes). Slices were rinsed with TBS and viewed using a confocal laser-scanning microscope (model TCS SP2; Leica Microsystems). Colocalization analysis was performed with a Multicolor software package (Leica Microsystems). All images were generated with Adobe Photoshop 7.0 (Adobe Systems).

RESULTS

A BLAST analysis of the murine PAT2 cDNA sequence with the expressed sequence tag (EST) data base revealed the presence of PAT2-EST clones obtained from the nervous system. Because in our previous report we could not detect the PAT2-mRNA in brain by using Northern blot analysis (12), we here applied RT-PCR analysis and show that the PAT2 mRNA was detectable in all nervous system regions analyzed. As shown in Fig. 1A, a 546-bp fragment was amplified from olfactory bulb, cortex, thalamus, cerebellum, brain stem, and spinal cord. The presence of the PAT2 protein in the brain was confirmed by using an anti-PAT2 antibody raised against 13 amino acids of the C-terminal sequence of the PAT2 protein. Western blot analysis using this antibody revealed the PAT2 protein to be present in the brain with an apparent molecular mass of 55 kDa (Fig. 1B). The specificity of the antibody was demonstrated by immunofluorescence studies in X. laevis oocytes after expression of PAT2 (Fig. 1, C–H) with water-injected oocytes as a negative control. Only in membranes of oocytes expressing

Fig. 2. Immunohistochemistry in cross-sections of the spinal cord (A-C) and parasagittal sections of the mouse brain with an anti-PAT2 anti**body** (D-I). Images A-C are in spinal cord. A, image of PAT2 immunoreactivity in spinal cord. gm, gray matter; wm, white matter. B, incubation with the antibody pre-absorbed with the antigenic peptide in an adjacent section. C, high power magnification of the ventral horn shows the presence of PAT2 in motoneurons and interneurons. Images D-I are in brain, D. image of PAT2 immunoreactivity in the whole brain. *Ob*, olfactory bulb; Cx, cerebral cortex; Hc, hippocampus; Cb, cerebellum; Bs, brain stem; Rh, rhinencephalon. E, pre-absorption of the anti-PAT2 antibody with the antigenic peptide showed no significant immunoreactivity on an adjacent section. High power magnifications of olfactory bulb (F), cerebral cortex(G), and brain stem(H) are shown. In all regions, pre-absorption of the anti-PAT2 antibody with the antigenic peptide abolished the immunoreactivity on an adjacent section, as shown in panel I for brain stem. Scale bars in B, C, E, and I apply to A and B, C, D-E, and F-I, respectively.



PAT2, a fluorescence signal was detected (Fig. 1C) that was blocked when the anti-PAT2 antibody was pre-absorbed with the antigenic peptide (Fig. 1G).

Immunolocalization of PAT2 in the Nervous System—Immunodetection studies revealed that the PAT2 protein is expressed in spinal cord and brain. As shown in Fig. 2A, in spinal cord, PAT2 is highly expressed in the gray matter and is not detectable in the white matter. The signals were abolished in an adjacent section by incubation with the antibody pre-absorbed with the antigenic peptide (Fig. 2B). In the anterior horn, PAT2 is present in motoneurons and interneurons (Fig. 2C) and in interneurons of the posterior horn (data not shown). In brain, PAT2 is found in various regions, with prominent expression in brain stem, cerebellum, hippocampus, hypothalamus, rhinencephalon, cerebral cortex, and olfactory bulb (Fig. 2D). In an adjacent section, signals were abolished by incubation of slices with the antibody pre-absorbed with the antigenic peptide (Fig. 2E). Colocalization studies using the glia marker GFAP (glial fibrillary acidic protein) showed that the PAT2 protein is solely detectable in neurons and not in astrocytes (data not shown). High power magnification demonstrates the expression of PAT2 in neurons of the mitral cell layer and interneurons in the olfactory bulb (Fig. 2F) as well as in neurons of the cerebral cortex (Fig. 2G) and large neurons in brainstem (Fig. 2H).

Cell-specific Expression of the PAT2 Protein—PAT2 is expressed in "NMDAergic" neurons in different regions of the central nervous system (Fig. 3A). PAT2 immunoreactivity is found in cells expressing the NMDA receptor subunit NR1, such as motoneurons and interneurons in the spinal cord and brainstem, Purkinje cells in the cerebellar cortex, neurons in the dentate gyrus, the CA1 and CA3 regions of the hippocampus, and neurons in different layers of the cerebral cortex (Fig. 3A). Moreover, a subset of neurons in the molecular layers of the hippocampal formation and the molecular and granular layers of the cerebellum show both NR1 and PAT2 immunoreactivity (Fig. 3, A and B). NR1 and PAT2 showed very similar staining intensities along the neuronal cell bodies; e.g. pyramidal cells of the hippocampal CA3 region stained stronger than the granule cells of the CA1 region. At higher magnification, a

partial subcellular colocalization of both proteins becomes evident (Fig. 3B). This subcellular colocalization is probably due to the expression of both proteins in the endoplasmic reticulum, as shown for PAT2 (see Fig. 4B) and previously for the NR1 subunit (27). No clear correlation of expression pattern was observed between PAT2 and the glycinergic marker protein GLYT2 (glycine transporter 2), the glycine-and-GABAergic marker gephyrin, and the GABAergic marker glutamate decarboxylase GAD65/67 (Fig. 3B). Whereas PAT2 is expressed at higher levels in Purkinje cells of the cerebellum, the glycine and GABAergic markers displayed higher expression levels in the molecular and/or granular layer. Such differential expression patterns in the colocalization of PAT2 with proteins of the glycine and GABAergic systems were also observed in other regions of the brain (data not shown), suggesting that PAT2 plays no role in the inhibitory glycine and GABAergic system. The missing correlation with the GABAergic system is not surprising, because GABA displays only a very low affinity to PAT2 (12).

Subcellular Localization of PAT2 in Neurons-We have shown previously that PAT2, unlike its paralog PAT1, is not detected in lysosomes and possesses a different subcellular distribution after expression in HeLa cells (12). As shown in Fig. 4A, in neurons of the brainstem, PAT2 is found mainly in the somata, predominantly in the cytoplasma and probably also partially in the plasma membrane. Its distribution, therefore, differs from the distribution pattern observed for PAT1. Colocalization studies using antibodies against different intracellular marker proteins in cross-sections of spinal cord were carried out for determining the subcellular compartments in which PAT2 is localized. Various regions of the nervous system have been examined, and in all cases the PAT2 protein did not colocalize with the Golgi marker protein GM130 or the early endosome marker protein EAA1 (Fig. 4B). On the other hand, it partly colocalized with the endoplasmic reticulum marker protein BiP/GRP78 and the early and recycling endosome marker protein Rab4. Quantification of PAT2 immunoreactive puncta indicated $\sim 34 \pm 3\%$ (n = 12) and $\sim 31 \pm 3\%$ (n = 15) colocalized with the endoplasmic reticulum marker protein and the recycling endosome marker protein, respectively. There-

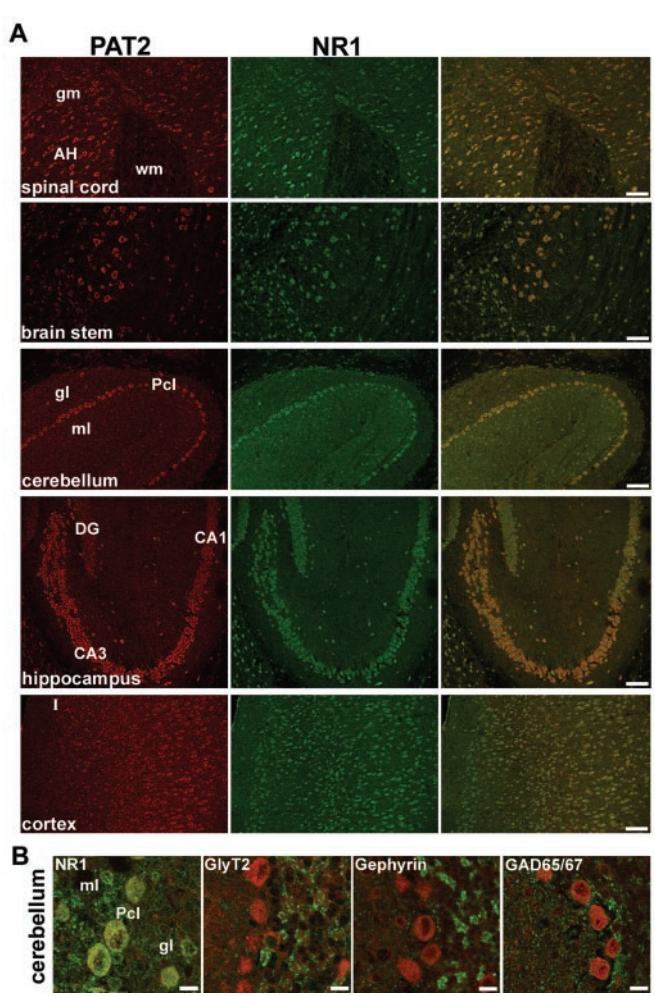


Fig. 3. Cell-specific expression of PAT2. A, confocal, laser-scanning, double immunofluorescence microscopy in parasagittal sections of different regions of the central nervous system with anti-PAT2 antibody (red) and anti-NR1 (green) antibody. The superimposed images are depicted on the right. B, higher resolution of double staining with anti-PAT2 (red) and anti-NR1, anti-GLYT2, anti-Gephyrin, or anti-GAD65/67 (green) antibodies. Colocalization appears in the superimposed images as yellow. gm, gray matter; wm, white matter; AH, anterior horn of spinal cord; gl, glomerular layer; ml, molecular layer; Pcl, Purkinje cell layer of cerebellum; DG, dentate gyrus, CA1, CA1 region; CA3, CA3 region of hippocampus; I, neuronal layer I of the cerebral cortex. Scale bars represent $80 \mu m$ (A) and $10 \mu m$ (B).

fore, PAT2 is found in endoplasmic reticulum and recycling endosomes, whereas the remaining fraction is localized in other compartments, including the cell membrane.

Functional Analysis of PAT2—Whereas in our previous report we demonstrated that PAT1 and PAT2 activities are generally dependent on extracellular pH and membrane potential (12), here we analyzed in more detail the kinetics of glycine transport (Fig. 5). Applying the TEVC technique in oocytes expressing PAT2, the glycine/H+ symport at saturating (10 mm) external glycine concentrations induced positive inward currents that increased by decreasing external pH from 9 to 7.5 (Fig. 5A). A further reduction of pH from 7.5 to 5.5 did not further enhance glycine currents (data not shown), and no current responses were observed in the water-injected oocytes. As shown in Fig. 5B, PAT2-mediated inward currents followed Michaelis-Menten kinetics when plotted as a function of apparent external proton concentration. The corresponding Eadie-Hofstee transformation (Fig. 5C) revealed an apparent halfmaximal proton activation constant of 4.7 \pm 0.2 nm and an $I_{
m max}$ of 462 \pm 12 nA. From this data it can be concluded that the

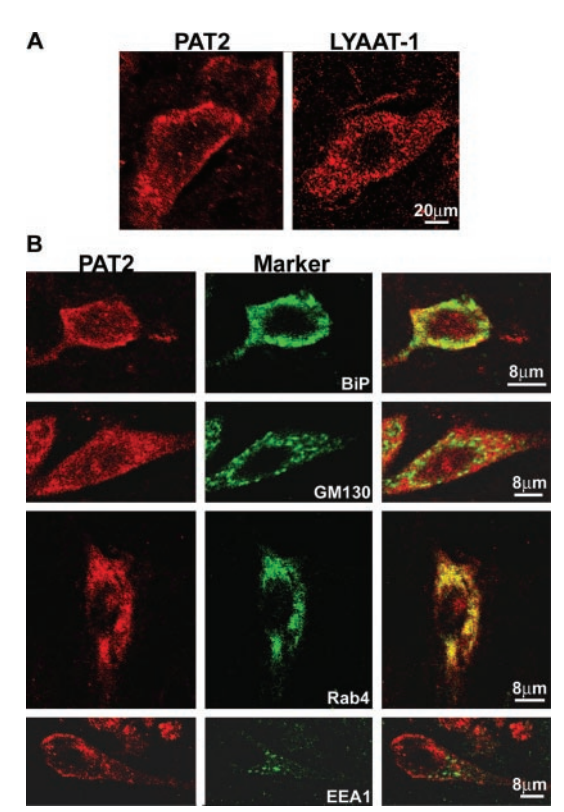


Fig. 4. Subcellular localization of PAT2 in neurons. A, immunofluorescence analysis with an anti-PAT2 (left) or an anti-LYAAT-1/PAT1 (right) antibody in adjacent brain stem slices. B, confocal, laser-scanning, double immunofluorescence microscopy in spinal cord cross-sections with anti-PAT2 antibody and antibodies against subcellular markers. PAT2 immunoreactivity is shown in red, and the marker immunoreactivity in green. The superimposed images are depicted on the right. BiP, endoplasmic reticulum marker; GM130, cis-Golgi marker; Rab4, early/recycling endosome marker; EEA1, early endosome marker.

external pH necessary for a half-maximal transport activation at a membrane potential of -60 mV is 8.3, suggesting that, at a physiological pH of 7.3 or in a more acidic environment, PAT2 operates already with a maximal transport rate.

Alterations in membrane potential play an important role in the brain in the regulation of membrane protein functions. Here we demonstrate that PAT2-mediated glycine currents are significantly altered by changes in the membrane potential (Fig. 5D). A hyperpolarization of the membrane increases inward currents, and voltage effects are more pronounced at higher glycine concentrations. Moreover, at low glycine concentrations (0.1 mm) a depolarization of the membrane induces outward currents represented by a reversed transport mode.

PAT2 Is Capable for Bidirectional Transport of Amino Acids—To characterize the capability of PAT2 for glycine efflux, we employed the giant patch clamp technique with membrane patches obtained from oocytes expressing PAT2. Positive outward currents were induced by 20 mm glycine (Fig. 6A) and showed pronounced voltage dependence. No comparable currents were obtained in water-injected oocytes (data not shown). The glycine-induced outward currents followed Michaelis-Menten kinetics as a function of substrate concentration (Fig. 6B), and the transformation of substrate-evoked currents according to Eadie-Hofstee revealed an apparent affinity (K_m) of glycine outward transport of 8.5 \pm 0.5 mm at a membrane potential of $-30~\rm mV$. Therefore, PAT2 can transport glycine bidirectionally with the direction of transport determined by membrane potential and/or the substrate/proton gradients.

Sarcosine Inhibition of Glycine Transport—Sarcosine is a

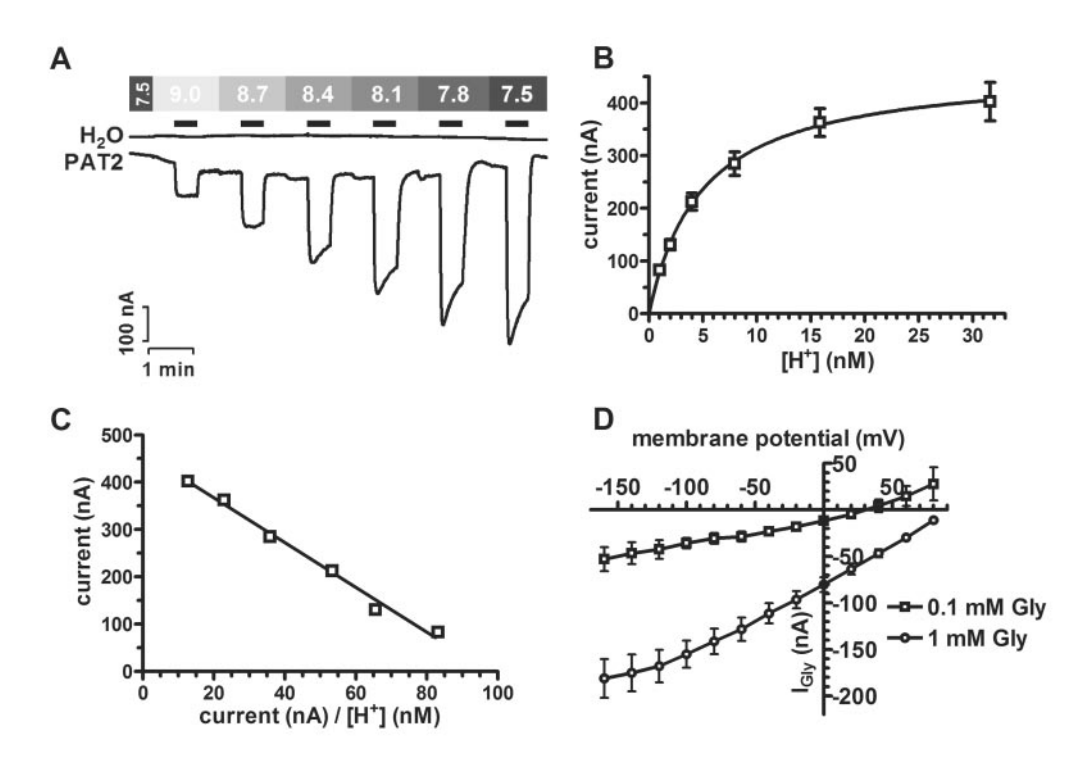


Fig. 5. **pH and membrane potential dependence of PAT2 activity.** A, oocytes injected with PAT2-cRNA or water clamped at -40 mV were perfused with incubation buffers adjusted to different pH rankings from 9 to 7.5 in the presence of 10 mM glycine. B, saturation kinetics of mediated currents by 10 mM glycine in the function of proton concentration (n = 9 oocytes) and the corresponding Eadie-Hofstee transformation (C). D, I-V relationship of glycine-evoked inward currents (n = 4 oocytes) at pH 6.5 and two different glycine concentrations, 0.1 and 1 mM.

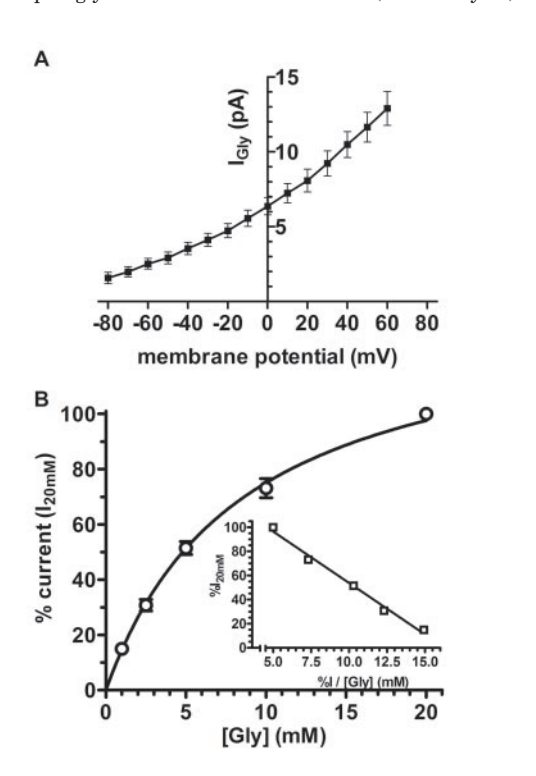


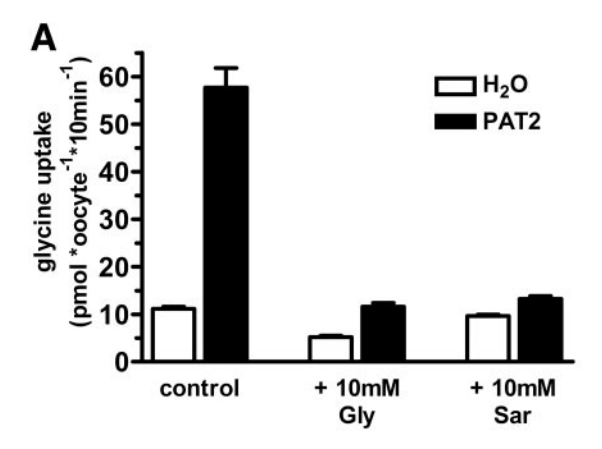
Fig. 6. Characteristics of the PAT2 outward transport mode using the inside-out giant patch clamp technique. A, I-V relationship of glycine-evoked outwards currents (20 mM) at pH 7.5 (n=4 oocytes). B, saturation kinetics of outward currents as a function of substrate concentrations and the corresponding Eadie-Hofstee transformation (inset).

known selective inhibitor of glycine transport in the brain (21, 22) and inhibits glycine influx mediated by the glycine transporter GLYT1 but not by the GLYT2 transporter. Here we

demonstrate that sarcosine is likewise able to inhibit glycine uptake mediated by PAT2. Flux studies performed with radio-labeled glycine in oocytes expressing PAT2 demonstrate that the uptake can be reduced by 10 mm sarcosine to almost the same extent as that obtained by 10 mm glycine as a competitor (Fig. 7A). In water-injected oocytes, no detectable uptake or inhibition was observed. Additionally, by using the TEVC technique we demonstrate that sarcosine induces inward currents that display saturation kinetics as a function of sarcosine concentration. The Eadie-Hofstee transformation of the substrate-evoked currents as a function of sarcosine concentration revealed an apparent K_m of $208 \pm 2~\mu\mathrm{M}$ and an I_{max} of $130 \pm 4~\mathrm{nA}$ (Fig. 7B).

DISCUSSION

All members of the mammalian subfamilies of the amino acid/auxin permease family are expressed in the nervous system, where they fulfill different physiological roles. Immunolocalization studies indicated the presence of VGAT in glycinergic, GABAergic, and mixed glycine and GABAergic synapses (4, 23). VGAT is responsible for the accumulation of the inhibitory neurotransmitters GABA and glycine in vesicles in presynaptic neurons. In the nervous system, the members of the system N/A subfamily show different cellular and subcellular expression patterns and are central for neurotransmission (14, 24, 25) by their role in the glutamate-glutamine cycle (14). SN1 is mainly responsible for the efflux of glutamine from the astrocytes, and the system A transporters 2 or 1 are responsible for its uptake into the neurons where it is converted to glutamate, allowing the recovery of glutamate to the presynaptic neurons. The proton/amino acid co-transporters PAT1 and PAT2 are present as well in the nervous system. PAT1 has been reported to be present in neurons of the hippocampus, cerebral cortex, cerebellum, and the thalamic and pontine nuclei (11, 19) with a more detailed cellular analysis reported recently (26). We demonstrate here by RT-PCR that the PAT2-mRNA is found in



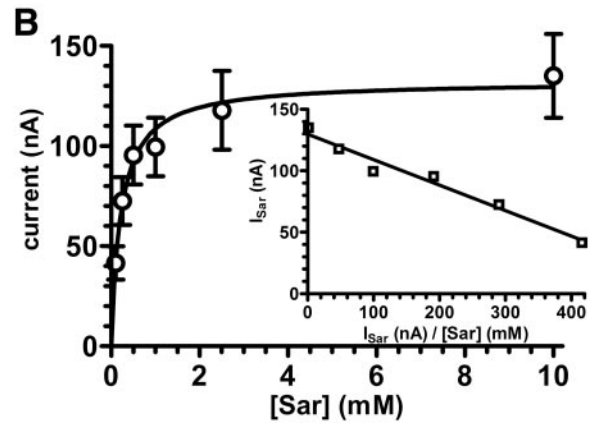


Fig. 7. Sarcosine (*Sar*) inhibits PAT2-mediated glycine transport. A, water and PAT2-cRNA-injected oocytes (n=8) were incubated with 100 μ M 3 H-glycine in the presence or absence of 10 mM sarcosine or 10 mM glycine. B, saturation kinetics of inward currents as a function of sarcosine concentrations at pH 6.5 and held at a membrane potential of -60 mV (n=5 oocytes), and the corresponding Eadie-Hofstee plot (*inset*).

all brain regions analyzed. The PAT2 protein was identified with an apparent molecular mass of 55 kDa and localized by immunodetection studies in spinal cord, brain stem, cerebellum, hippocampus, hypothalamus, rhinencephalon, cerebral cortex, and the olfactory bulb. By colocalization with a glial marker protein in various brain regions, PAT2 was exclusively found in neurons similar to its orthologue PAT1.

It has been shown that PAT1 is expressed particularly in regions rich in glutamatergic neurons (11, 19, 26). Here, we show that the cell-specific expression pattern of PAT2 strongly resembles that of the NMDA receptor subunit NR1 (27, 28). The NR1 subunit forms, together with the different NR2 or NR3 subunits, the hetero-oligomeric NMDA subtype of ionotropic glutamate receptors. They serve critical functions in several processes in the central nervous system, including neuronal development, plasticity, and neurodegeneration (29). Receptor activation usually requires the two agonists glutamate and glycine (30). However, recently it has been shown that NMDA receptors comprised of the NR1 and NR3A/B subunits require solely glycine for activation (31). The observed overlapping cell type-specific expression pattern of PAT2 and NR1 suggests, but does not prove, a functional role of PAT2 in the excitatory glycinergic neurotransmission.

Although the transport mode and the general distribution pattern of the two PAT transporters are similar, there are marked differences in their subcellular localization and functional characteristics. PAT1 has broader substrate specificity than PAT2 and can, in addition to small amino acids, also transport GABA and other amino acid derivatives (11, 12, 17).

PAT2, in contrast, is restricted to alanine, glycine, and proline, but has much higher substrate affinities than PAT1 (µM versus mm). PAT1 and PAT2 also differ in their subcellular localization. PAT1 was shown to be localized in the lysosomes and, to a small extent, in the plasma membrane of neurons (11, 19), and a recent report demonstrated that PAT2 is not present in lysosomes in teased fibers (32). When PAT2 is expressed in HeLa cells, the protein is localized in the plasma membrane and intracellular compartments but not in lysosomes (12). Here we show that, within the cell, PAT2 is present in the endoplasmic reticulum and in recycling endosomes. PAT2, as a high affinity/low capacity system, may therefore play a role in the export of amino acids from the endosomes to the cytoplasm, whereas PAT1, as the low affinity/high capacity system, may serve for lysosomal export of amino acids derived from protein breakdown. Both transporters act as rheogenic H⁺-coupled symporters and, therefore, changes in the extracellular pH alter their function. PAT1 activity is strongly pH-dependent, and its maximal transport rate is reached at an external pH of 5.5-6. Here we show that PAT2 operates with full activity at physiological pH (\leq 7.5), and its activity declines when external pH becomes alkaline. Both transporters therefore show maximal transport rates at pH conditions characteristic for those in recycling endosomes (around pH 6.7) and lysosomes (\sim 5.5).

With its presence in recycling endosomes, PAT2 may also, on occasion, reach the plasma membrane where it could serve as an import or export system for glycine or the other amino acids. Previous studies on the kinetics of glycine transport in the rat central nervous system already suggest the existence of a low and a high affinity transport system for glycine with apparent K_m values of ~ 800 and $26~\mu\mathrm{M}$, respectively (33). The two cloned glycine transport systems, GLYT1 and GLYT2, are considered to represent the molecular entities of the high affinity glycine transport pathway (21, 22, 34-36), whereas the low affinity glycine transport system, shown to be sodium independent (37), is not yet known. By its apparent affinity of 590 \pm 4 μ M for glycine (12), it may be speculated that PAT2 represents that low affinity glycine transport mechanism. In addition, glycine transport in brain is inhibited by sarcosine. Whereas the GLYT1 transporter displays a IC_{50} value of around 100 μM for sarcosine inhibition of glycine influx and sarcosine transport (38), PAT2 likewise transports sarcosine with an apparent substrate of 208 μ M and shows glycine transport inhibition in the presence of sarcosine. As demonstrated by heterologous expression in oocytes, PAT2 activity is affected by membrane potential, and hyperpolarization increases glycine-evoked currents. In inhibitory synapses, this could have a physiological role by enhancing glycine transport via PAT2 after membrane hyperpolarization induced by activation of the glycine receptor. We also demonstrate another feature of PAT2, and this is its ability for bidirectional glycine transport. A depolarization of the plasma membrane results in an increased outward current when glycine is provided on the cytosolic side. Although the apparent affinity of glycine for binding to the internal substrate binding domain is lower than that on the outside, a glycine efflux via PAT2 could occur when intracellular glycine concentrations rise. In glutamatergic neurons, the coactivation of the NMDA receptors by glycine induces a depolarization of the neuronal membrane that could initiate a reversed glycine transport by PAT2. This non-vesicular release could then contribute to a sustained glycine signal, as proposed for selected synapses (39). This would be of importance for some glycinergic nerve terminals that failed to show the presence of VGAT. Transmembrane concentration gradients of its substrates and membrane potential finally determine the direction and velocity of amino acid transport mediated by PAT2.

In conclusion, PAT2 is present in the nervous system where it, together with PAT1, may contribute to the handling of amino acids such as glycine, alanine, and proline in the endosomal/lysosomal system, but possibly also in the plasma membrane. At present, we cannot answer the question of whether PAT2-mediated transport of its specific amino acid substrates is of physiological importance in the mammalian brain, but PAT2 is a candidate protein for a still missing low affinity-type glycine transporter in the central nervous system. Together with GLYT1 and GLYT2, PAT2 could be responsible for the regulation of intracellular and extracellular concentrations of glycine that modulate glycine and glutamatergic neurotransmission.

Acknowledgment—We thank B. Giros for providing the anti-LYAAT1 antibody.

REFERENCES

- Saier, M. H., Jr. (2000) Microbiology 146, 1775–1795
- Young, G. B., Jack, D. L., Smith, D. W., and Saier, M. H., Jr. (1999) Biochim. Biophys. Acta 1415, 306–322
- Boll, M., Foltz, M., Rubio-Aliaga, I., and Daniel, H. (2003) Genomics 82, 47–56
 McIntire, S. H., Reimer, R. J., Schuske, K., Edwards, R. H., and Jorgensen,
- E. M. (1997) Nature 389, 870–876
 Sagne, C., El Mestikawy, S., Isambert, M. F., Hamon, M., Henry, J. P., Giros,
- B., and Gasnier, B. (1997) FEBS Lett. 417, 177–183
 6. Varoqui, H., Zhu, H., Yao, D., Ming, H., and Erickson, J. D. (2000) J. Biol.
- Chem. 275, 4049-4054
 Sugawara, M., Nakanishi, T., Fei, Y. J., Huang, W., Ganapathy, M. E.,
- Sugawara, M., Nakanishi, T., Fei, Y. J., Huang, W., Ganapathy, M. E., Leibach, F. H., and Ganapathy, V. (2000) J. Biol. Chem. 275, 16473–16477
 Sugawara, M., Nakanishi, T., Fei, Y. J., Martindale, R. G., Ganapathy, M. E.,
- Sugawara, M., Nakanishi, T., Fei, Y. J., Martindale, R. G., Ganapathy, M. E., Leibach, F. H., and Ganapathy, V. (2000) Biochim. Biophys. Acta, 1509, 7–13
- Chaudhry, F. A., Reimer, R. J., Krizaj, D., Barber, D., Storm-Mathisen, J., Copemhagen, D. R., and Edwards, R. H. (1999) Cell 99, 769–780
- Nakanishi, T., Sugawara, M., Huang, W., Martindale, R. G., Leibach, F. H., Ganapahty, M. E., Prasad, P. D., and Ganapathy, V. (2001) Biochem. Biophys. Res. Commun. 281, 1343–1348
- Sagne, C., Agulhon, C., Ravassard, P., Darmon, M., Hamon, M., El Mestikawy, S., Gasnier, B., and Giros, B. (2001) Proc. Natl. Acad. Sci. U. S. A. 98, 7206-7211
- Boll, M., Foltz, M., Rubio-Aliaga, I., Kottra, G., and Daniel, H. (2002) J. Biol. Chem. 277, 22966–22973
- Nakanishi, T., Kekuda, R., Fei, Y. J., Hatanaka, T., Sugawara, M., Martindale, R. G., Leibach, F. H., Prasad, P. D., and Ganapathy, V. (2001) Am. J. Physiol. 281, C1757–C1768
- 14. Chaudrhy, F. A., Reimer, R. J., and Edwards, R. H. (2002) J. Cell Biol. 157,

- 349-355
- Chaudhry, F. A., Schmitz, D., Reimer, R. J., Larsson, P., Gray, A. T., Nicoll, R., Kavanaugh, M., and Edwards, R. H. (2002) J. Neurosci. 22, 62–72
- Boll, M., Daniel, H., and Gasnier, B. (2004) Pflügers Arch. DOI: 10.1007/s00424-003-1073-4
- Boll, M., Foltz, M., Anderson, C. M. H., Oechsler, C., Kottra, G., Thwaites, D. T., and Daniel, H. (2003) Mol. Membr. Biol. 20, 261–269
- Chen, Z., Fei, Y.-J., Anderson, C. M. H., Wake, K. A., Miyauchi, S., Huang, W., Thwaites, D. T., and Ganapathy, V. (2003) J. Physiol. 546, 349–361
- Wreden, C. C., Johnson, J., Tran, C., Seal, R. P., Copenhagen, D. R., Reimer, R. J., and Edwards, R. H. (2003) J. Neurosci. 23, 1265–1275
- 20. Kottra, G., and Daniel, H. (2001) J. Physiol. 536, 495-503
- Smith, K. E., Borden, L. A., Hartig, P. R., Branchek, T., and Weinshank, R. L. (1992) Neuron 8, 927–935
- Liu, Q. R., Lopez-Corcuera, B., Mandiyan, S., Nelson, H., and Nelson, N. (1993)
 J. Biol. Chem. 268, 22802–22808
- Dumolin, A., Rostaing, P., Bedet, C., Levi, S., Isambert, M. F., Henry, J. P., Triller, A., and Gasnier, B. (1999) J. Cell Sci. 112, 22802–22808
- Reimer, R. J., Chaudhry, F. A., Gray, A. T., and Edwards, R. H. (2000) Proc. Natl. Acad. Sci. U. S. A. 97, 7715–7720
- Armano, S., Coco, S., Bacci, A., Pravettoni, E., Schenk, U., Verderio, C., Varoqui, H., Erickson, J. D., and Matteoli, M. (2002) J. Biol. Chem. 277, 10467–10473
- Agulhon, C., Rostaing, P., Ravassard, P., Sagne, C., Triller, A., and Giros, B. (2003) J. Comp. Neurol. 462, 71–89
- Petralia, R. S., Yokotani, N., and Wenthold, R. J. (1994) J. Neurosci. 14, 667–696
- Moriyoshi, K., Masu, M., Ishii, T., Shigemoto, R., Mizuno, N., and Nakanishi, S. (1991) *Nature* 354, 31–37
- Cull-Candy, S., Brickley, S., and Farrant, M. (2001) Curr. Opin. Neurobiol. 11, 327–335
- Monyer, H., Sprengel, R., Schoepfer, R., Herb, A., Higuchi, M., Lomeli, H., Burnashev, N., Sakmann, B., and Seeburg, P. H. (1992) Science 256, 1217–1221
- Chatterton, J. E., Awobuluyi, M., Premkumar, L. S., Takahashi, H., Talantova, M., Shin, Y., Cui, J., Tu, S., Sevarino, K. A., Nakanishi, N., Tong, G., Lipton, S. A., and Zhang, D. (2002) Nature 415, 793–798
- Bermingham, J. R., Jr., Shumas, S., Whisenhunt, T., Sirkowski, E. E., O'Connell, S., Scherer, S. S., and Rosenfeld, M. G. (2002) J. Neurosci. 22, 10217–10231
- 33. Logan, W. J., and Snyder, S. H. (1971) Nature 234, 297–299
- Guastella, J., Brecha, N., Weigmann, C., Lester, H. A., and Davison, N. (1992)
 Proc. Natl. Acad. Sci. U. S. A. 89, 7189–7193
- 35. Liu, Q. R., Nelson, H., Mandiyan, S., Lopez-Corcuera, B., and Nelson, N. (1992) $FEBS\ Lett.\ 305,\ 110-114$
- Zafra, F., Aragon, C., Olivares, L., Danbolt, N. C., Gimenez, C., and Storm-Mathisen, J. (1995) J. Neurosci. 15, 3952–3969
- 37. Bennett, J. P., Jr., Logan, W. J., and Synder, S. H. (1972) Science 178, 997-999
- 38. Supplisson, S., and Bergman, C. (1997) J. Neurosci. 17, 4580–4590
- 39. Attwell, D., and Bergman, C. (1993) Neuron 11, 401-407

The Proton/Amino Acid Cotransporter PAT2 Is Expressed in Neurons with a Different Subcellular Localization than Its Paralog PAT1

Isabel Rubio-Aliaga, Michael Boll, Daniela M. Vogt Weisenhorn, Martin Foltz, Gabor Kottra and Hannelore Daniel

J. Biol. Chem. 2004, 279:2754-2760. doi: 10.1074/jbc.M305556200 originally published online November 3, 2003

Access the most updated version of this article at doi: 10.1074/jbc.M305556200

Alerts:

- · When this article is cited
- When a correction for this article is posted

Click here to choose from all of JBC's e-mail alerts

This article cites 38 references, 17 of which can be accessed free at http://www.jbc.org/content/279/4/2754.full.html#ref-list-1